Available online at www.sciencedirect.com

ScienceDirect

journal homepage: www.elsevier.com/locate/he

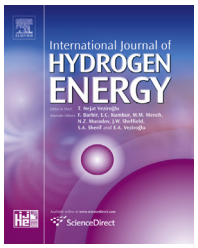

Zirconium phosphate based proton conducting membrane for DMFC application

Jay Pandey [a], *Murali Mohan Seepana* [b], *Anupam Shukla* [a,*]

[a] *Department of Chemical Engineering, Indian Institute of Technology Delhi, Hauz Khas, New Delhi 110016, India*
[b] *Department of Chemical Engineering, National Institute of Technology, Warangal 506004, Andhra Pradesh, India*

ARTICLE INFO

Article history:
Received 9 October 2014
Received in revised form
12 May 2015
Accepted 16 May 2015
Available online 11 June 2015

Keywords:
Ion-exchange membrane
Zirconium phosphate
PVDF
Methanol crossover
DMFC

ABSTRACT

A proton conducting poly(vinylidene fluoride) (PVDF) supported zirconium phosphate (ZrP) ion-exchange membrane (ZrP/PVDF) was synthesized for potential application in DMFC by filling the pores of a PVDF film with in-situ grown ZrP particles. Presence of labile protons attached to P=O group was confirmed from ^{1}H NMR and FT-IR characterizations. SEM micrographs showed defect-free top surface. The thermal stability and mechanical strength of the ZrP/PVDF membrane was better than Nafion-117. Water to methanol uptake ratio was higher while methanol cross-over for ZRP/PVDF membrane was lower than Nafion-117. Membrane possessed fair electrochemical properties; 0.85 static counter-ion transport number, 0.76 meqg^{-1} ion exchange capacity and 1.25 mScm^{-1} proton conductivity at 30 °C. DMFC performance of the synthesized membrane at 35 °C was compared with the Nafion-117. DMFC studies were also done at different operating conditions and the maximum peak power density was 32.3 mWcm^{-2} at 60 °C, 1 M methanol concentration and 60% relative humidity.

Introduction

In the recent past, interest in advanced functional materials, like membranes, electro-catalysts, and bipolar plates, has gained much attention due to emergence of various energy devices like fuel cell, batteries, sensors etc. Among all these devices, fuel cell particularly the direct methanol fuel cell (DMFC) has unique features of easy operation, higher energy density with low emission [1]. Membrane's properties considerably affect the DMFC performance. At present, polymeric membranes have been found to be the most appropriate for DMFC applications; however their poor thermal stability and deterioration in performance at elevated temperature (>80 °C) has led to the search for alternative membranes.

Inorganic-organic ion-exchange membranes composed of organic support with distributed inorganic phase having functional (ionic) groups possess enhanced physical and chemical properties compared to both organic and purely inorganic membranes and have potential to be used in DMFC. The inorganic phase is selected on the basis of its ion exchange capacity (IEC) and proton conductivity. A type of inorganic ion-exchangers, called fast proton conductors have gained interest in recent times. These materials are acid salts of tetravalent metal and their general chemical formula is [M(IV) HPO_4 nH_2O] where, M is the tetravalent metal e.g., Sn, Zr, Ti. Protons (H^+) of the hydroxyl group (–OH) structurally

* *Corresponding author*. Tel.: +91 11 26596290; fax: +91 11 26581120.
E-mail address: anupam@chemical.iitd.ac.in (A. Shukla).
http://dx.doi.org/10.1016/j.ijhydene.2015.05.117

bound to the metal M acts as ion-exchangeable sites [2,3] and enable proton conduction. A number of small cations (Li^+, Na^+, Ca^{2+} etc.) can be exchanged with H^+ providing high IEC [4]. Protons can easily move on surface containing hydrated −OH groups [5]. Zirconium phosphate (ZrP) is one of the most widely studied fast proton conductors because it has high IEC (6.64 $meqg^{-1}$) [3]. Also, ZrP is thermally stabile up to 450 °C. However, it has very low proton conductivity, in the range of 10^{-5}–10^{-6} Scm^{-1} [5].

Recent literature reported synthesis of inorganic-organic composite membranes by impregnation of porous support, of polymeric materials such as poly(vinylidene fluoride) (PVDF), poly(tetrafluoro ethylene) (PTFE), poly(propylene) (PP), poly(ethersulfone) (PES), with a colloidal suspension of inorganic ion exchangers [6]. It was pointed out by Alberti et al. [7] that the transfer of the colloidal dispersion of ZrP particles into a polymeric matrix enables proper dispersion of the inorganic particles due to their small particle size (ranging from nano to micrometers). The advantages of such composite inorganic-organic membranes include low cost, good mechanical strength in both wet as well as dry state, and good thermal stability. In addition, it is possible to obtain membranes much thinner than Nafion-117 (175 μm) yet maintaining comparable mechanical strength and methanol crossover. Thinner dimensions leads to lower areal resistance of the membrane. ZrP based membranes have been reported in literature [8–10]. Some of them have shown that hybridization of Nafion membrane with inorganic ZrP reduces methanol crossover of the membrane.

In this work, synthesis of ZrP based proton conducting membrane is described. Synthesis was carried out by impregnating porous polymeric PVDF film of sub-micron pore size with in-situ grown ZrP particles. Synthesized ZrP/PVDF membrane was characterized using various physico-chemical (^{1}H NMR, XRD, FT-IR, SEM, stability test, water uptake) and electrochemical characterization techniques (Transport number, IEC, proton conductivity). Methanol crossover was measured and the membrane's performance in DMFC was compared with that of Nafion-117.

Experimental

Materials

Porous PVDF film (pore size 0.22 μm, thickness 50 μm) was procured from Rankem Pvt. Ltd., India. Zirconyl oxycholoride ($ZrOCl_2$ $8H_2O$) and ortho-phosphoric acid (H_3PO_4) were purchased from Central Drug House (CDH), India. Other chemicals like methanol, sodium chloride, acetone, ethanol, hydrogen peroxide, hydrogen chloride and sulfuric acid were purchased from Merck Ltd., India. All the chemicals were of AR grade and triple de-ionized water was used for all the experiments.

Synthesis

ZrP ion-exchanger

ZrP powder was prepared by adding 10 ml of 5 wt.% zirconyl oxychloride (salt precursor of zirconium ion (Zr^{4+})) to 10 ml of 0.5 M H_3PO_4 solution while stirring. A few drops of HCl acid were also added to the solution to maintain the pH between 2 and 3. The prepared solution was stirred for 2 h at room temperature during which it turned milky. It was then filtered (using Whatman filter, Grade 1) to obtain white precipitate. The obtained white precipitate was washed multiple times with water to remove excess acid followed by heating at 120 °C for 12 h to get the ZrP powder. The prepared ZrP powder was characterised using FT-IR, particle size analyzer (PSA) and XRD.

ZrP/PVDF membrane

Membrane was synthesized in two steps. First a porous PVDF film was immersed in 5 wt.% $ZrOCl_2$ aqueous solution at 80 °C for 6 h. In the second step, after removing excess solution from the surface, the $ZrOCl_2$ impregnated PVDF film was immersed in 0.5 M H_3PO_4 solution containing few drops of HCl for 48 h for the in-situ formation of ZrP inside the pores of the PVDF film. This was followed by heat treatment at 120 °C for 12 h.

Characterization

Characterization of ZrP

^{1}H-MAS NMR spectroscopy of the synthesized ZrP sol was done on a Bruker Electrospin machine (make: Bruker USA, model: 300 MHz) to determine the state of protons (H^+) present in the sol. For this DMSO-d_6 (di-methyl sulphoxide dissolved in deuterated water) was used as an NMR solvent. The chemical shifts (up-fields and down-fields) and peaks were referenced to tetramethoxysilane (TMS) used as an external standard. The particle size distribution (PSD) and zeta potential of ZrP particles of the sol was measured at 30 °C and 60% RH on a particle size analyzer (make: Malvern Instruments UK, model: S90). The FT-IR of the ZrP powder, obtained by drying the ZrP sol, was measured on a spectrometer (make: Thermo Nicolet USA, model: 6700) in transmittance mode over wavenumber range of 500–4000 cm^{-1}. For this purpose, a pellet was made by mixing the powered sol with KBr and then it was heat treated at 100 °C for 2 h to remove the moisture. XRD of the powdered form of the sol was done on an X-ray diffractometer (make: Philips Pro Xpert The Netherlands, model: PW 3040) operated at 45 kV and 40 mA with monochromatic Cu K_α radiation. The two theta (2θ) range was kept between 10 and 60° with step size of 0.02°. Both XRD and FT-IR test were performed at 30 °C and 60% RH.

Characterization of ZrP/PVDF membrane

XRD. XRD of the membrane was done in a way similar to that of the powdered sol described above.

Scanning electron microscopy-energy dispersive X-ray spectroscopy (SEM-EDS)

SEM (make: ZEISS Germany, model: EVO-50) was used to study the surface morphology of PVDF film and ZrP/PVDF membrane. Samples were dried at 150 °C for 2 h to remove the moisture and then coated with gold under vacuum before performing the SEM experiment. Elemental composition of the synthesized membrane was determined using EDS.

Thermo-gravimetric analysis/differential scanning calorimetry (TGA/DSC)

Loss in weight of the membrane and heat flow with rising temperature was measured using TGA/DSC analyzer (make: TA Instruments USA, model: TA-Q600). 10 mg of membrane sample was used and experiment was carried out with air flow rate of 200 ml min^{-1}. Temperature was increased up to 800 °C at the rate of 10 °C min^{-1}. Heat involved and released (endothermic and exothermic reactions) was measured using DSC. TGA was also carried out for Nafion-117 membrane under identical conditions.

Tensile test

Tensile strength of the membrane was measured at room temperature (30 °C) and 60% RH on an Instron Tester (make: Instron Microtensile Tester Singapore, Model: 5848) as per ASTM standard D4595 (at the crosshead speed of 5 mm min^{-1} under test load of 10 N). Size of the specimen was 15 mm × 5 mm. The tensile strength was measured in dry state. Three measurements were made and the average value is reported.

Oxidative stability test

Oxidative stability of membrane sample was determined by immersing it in hot Fenton's reagent (3% H_2O_2 aqueous solution containing 2 ppm $FeSO_4$) at 80 °C. Weight loss of the membrane in hot Fenton's reagent was measured every 1 h and till the sample started to break or dissolve in solution.

Water and methanol uptake

Membrane sample was immersed in de-ionized water for 24 h after which it was taken out from the water. The water on the surface of the sample was removed by wiping with tissue paper and the sample was weighed immediately. Water uptake was calculated as,

$$\text{Water uptake}(\%) = \frac{(W_{wet} - W_{dry})}{W_{dry}} \times 100 \quad (1)$$

where, W_{wet} and W_{dry} are the weights of membrane sample in wet and dry states.

Identical procedure was used for methanol uptake. Instead of water, membrane was immersed in methanol. All the measurements were carried out at room temperature (30 °C) and 60% RH.

Transport number

Transport number of the membrane was calculated from membrane potential measurement done using the diffusion cell technique. The diffusion cell comprised of two compartments of volume 27 cm^3 each, separated by the membrane of circular shape with an exposed area of 12.56 cm^2. Ag/AgCl electrodes were placed inside each compartment of the diffusion cell. Aqueous NaCl solutions of two different concentrations were used for the experiments. Membrane was equilibrated with NaCl solution of lower concentration for 24 h and then mounted on the cell. Lower concentration NaCl solution (0.01 M) was filled in the compartment on the support side of the membrane while the higher concentration solution (0.1 M) was filled in the compartment on the active side of the membrane. Potential difference between the bulk of liquids in the two compartments was measured using Ag/AgCl electrodes and a multimeter (make: Mastech Inc. India, model: 3900). Transport number for the cation (Na^+) inside the membrane was calculated using Plank-Henderson equation given below [11],

$$E_m = \frac{RT}{nF}(2t_+ - 1)\ln\frac{C_1}{C_2} \quad (2)$$

where, E_m is the membrane potential (V), t_+ is the transport number for Na^+ ion, C_1 is the higher concentration (0.1 M) and C_2 is the lower concentration (0.01 M) of NaCl. R is the universal gas constant (8.314 $Jmol^{-1}K^{-1}$), F is the Faraday's constant (96,485 $Cmol^{-1}$) and T is temperature (K).

IEC

IEC was determined using acid-base titration method using method reported in literature [12]. The synthesized membrane was kept in 100 ml of 0.1 M NaCl solution for 24 h to allow the exchange of H^+ ions with Na^+. The solution was then back-titrated with 0.5 M NaOH using phenolphthalein as an indicator. IEC ($meqg^{-1}$) was calculated as,

$$IEC = \frac{V_{NaOH}M_{NaOH}}{W_{dry}} \quad (3)$$

where, V_{NaOH} and M_{NaOH} is volume and molarity of NaOH, W_{dry} is the weight of dry membrane (g). The membrane sample was regenerated using aqueous 0.5 M HCl solution. Three cycles of ion-exchanging and regeneration were carried out and the reported values are for the third cycle.

Proton conductivity

Proton conductivity of the membrane at 30 °C and 60% RH was calculated from measured values of resistance and thickness. Resistance of the two-compartment cell (described above for membrane potential measurement) with and without membrane was measured on a Potentiostat/Galvanostat with frequency response analyzer (make: Gamry Instrument Inc. USA, model: Reference-600) using two-probe impedance method. Membrane was equilibrated with 0.5 M HCl solution for 12 h before measurement. Both the compartments were filled with 0.5 M solution of HCl. 10 mV amplitude ac signal was scanned from 1 mHz to 1 MHz. Impedance value at zero phase angle was taken as the resistance of the cell. Membrane resistance (R_m) was obtained from difference of resistance values of cell, with and without membrane. The specific conductivity (σ) and areal resistance (R) of the membrane was calculated as,

$$\sigma = \frac{L}{R_m A} \quad (4)$$

$$R_{areal} = \frac{L}{\sigma} \quad (5)$$

where, R_m is resistance (Ω), L is the thickness (cm), A is the exposed area (cm^2) and R_{areal} is the areal resistance (Ω–cm^2) of the membrane.

Methanol crossover

A two-compartment diffusion cell was used to measure the permeation of methanol through synthesized membrane.

Both compartments, of capacity of 20 cm^3 each, had provision for stirring. Initially, one compartment (A) contained an aqueous solution of methanol (1 M) while the other (B) contained de-ionized water. Liquids in both the compartment were continuously stirred during the experiments in order to maintain uniform concentration throughout the compartment. The concentration of methanol in compartment B was determined at different times using a gas chromatograph (Make: Nucon Gas Chromatograph India, Model: 5765) equipped with flame ion detector (FID). Methanol permeability (P) at 30 °C and 60% RH was calculated by the below given formula reported in literature [13],

$$P = \frac{lV_B}{At} \ln \frac{C_B^o - C_A}{C_B^t - C_A} \quad (6)$$

where C_B^o is the initial methanol concentration in compartment B, C_B^t is the methanol concentration in compartment B at a particular time t, C_A the methanol concentration in compartment A and V_B the volume of compartment B, A is the exposed area of the membrane and l is the thickness of the membrane.

Single cell DMFC test

MEA was prepared by the hot pressing, at 60 °C and 10 MPa pressure for 5 min, the membrane between two commercially available (Johnson Matthey catalysts, Alfa Aesar India Ltd., Hyderabad) catalyst layers. Anode catalyst (Pt/C) loading was 2 $mgcm^{-2}$ and cathode catalyst (Pt–Ru/C) loading was 2 $mgcm^{-2}$. Polarization curve were measured on a 25 cm^2 DMFC single cell (Electrochem Inc. USA) with 1 M methanol flow rate of 3 ml min^{-1} on anode side and air flow rate of 300 ml min^{-1} on cathode side. Temperature was kept 35 °C, and relative humidity of air was maintained at 60%.

Results and discussion

Impregnation technique was used for the synthesis of ZrP/PVDF membrane. In-situ formation of the inorganic ZrP in the pores of PVDF polymeric matrix resulted into final inorganic-organic membrane.

Characterization of ZrP

^{1}H-NMR-MAS

Liquid ^{1}H-NMR-MAS for the ZrP, shown in Fig. 1, was carried out to determine change in state of protons. This change in proton state is an indication of presence labile protons associated with ZrP. The sharp peak at ppm value of 2.04 was due to water present in ZrP and peak at ppm value of 4.57 was due to DMSO solvent. The peak at ppm value of 1.07 was due to TMS used as standard component. Small peaks at ppm values of 2.49 and 3.43 were due to presence of protons attached to the P═O group forming POH group [14].

Particle size distribution

Fig. 2 shows a monodispersed particle size distribution (volume %) of ZrP particles. The average size of the ZrP particles, determined from dynamic light scattering (DLS) technique, was 134.1 nm. Zeta potential of the particles was −18 mV.

FT-IR analysis

FT-IR was used to see the presence of characteristic peaks associated with functional groups of ZrP (to confirm formation of ZrP) and also to see the shift in the positions of some of these peaks due to hydrogen bonds formation at the P═O group. FT-IR spectrum of the ZrP powder is shown in Fig. 3. The peak at 1635 cm^{-1} was due the H–O–H stretching. The other two peaks at 530 cm^{-1} and 1035 cm^{-1} were due to $-PO_4^{3-}$ and P═O groups respectively. The peak obtained at wavenumber 1400 cm^{-1} was due to the P–OH bond which confirms the formation of α-zirconium phosphate ($Zr(HPO_4)_2\ H_2O$) [15]. The broad peak at the 3400 cm^{-1} was due to –OH stretching and it indicated presence of structurally bound water in ZrP.

ZrP structure from XRD

XRD pattern of the powdered ZrP is shown in the Fig. 4. The XRD pattern was compared with the ICDD patterns and all the peaks matched with those of α-ZrP. The shar peaks for the synthesized ZrP indicated crystalline nature of the synthesized ZrP.

Thermal stability analysis using TGA/DSC

The TGA and DSC curves for the synthesized ZrP powder are shown in Fig. 5. The TGA curve showed initial weight loss (10%) up to 100 °C due to the loss of unbound moisture or surface water and corresponding endothermic peak was observed. On the other hand, small endothermic peak at 250 °C was due to loss of structurally bound water present in ZrP [16] and corresponding weight loss of 5% was observed between 120 °C and 250 °C. The weight loss at 300 °C is attributed to the condensation of mono-hydrogen phosphate to pyrophosphate. Little loss in weight was observed after 600 °C. The analysis showed that the ZrP particles are stable up to 450 °C and showed high residual weight even at a very high temperature.

ZrP/PVDF membrane characterization

Phase analysis using XRD

XRD patterns of the PVDF film and ZrP/PVDF membrane are shown in the Fig. 6. PVDF film did not show any sharp peaks indicating its amorphous nature. On the other hand the membrane showed sharp peaks indicating the presence of impregnated ZrP particles in the porous PVDF film. The presence of the ZrP particles in the membrane introduces the ion-exchange phase and imparts ion selective permeation property to the membrane.

SEM-EDS

SEM images of the PVDF film and the membranes (ZrP/PVDF) obtained at different impregnation (in-situ synthesis) times are shown in Fig. 7(a), (b) and (c) respectively. Fig. 7(a), the top view of PVDF film, shows distribution of the pores with surface pore size about 0.22 μm. SEM images of the membranes with impregnation times of 12 h and 48 h (Fig. 7(b) and (c) respectively) shows ZrP particles embedded on PVDF film. The heat treated membrane has no pores of micron size

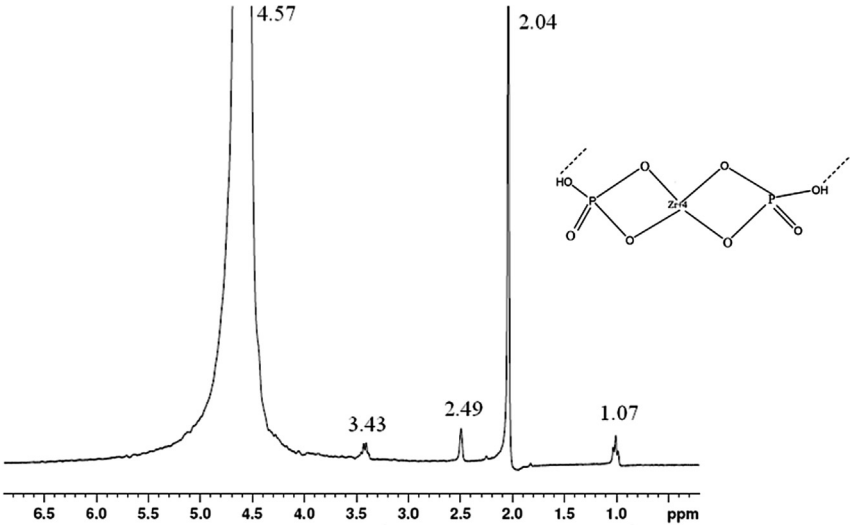

Fig. 1 – ^{1}H NMR for the synthesized ZrP showing the brønsted acidity behavior of hydroxyl groups present in the ZrP.

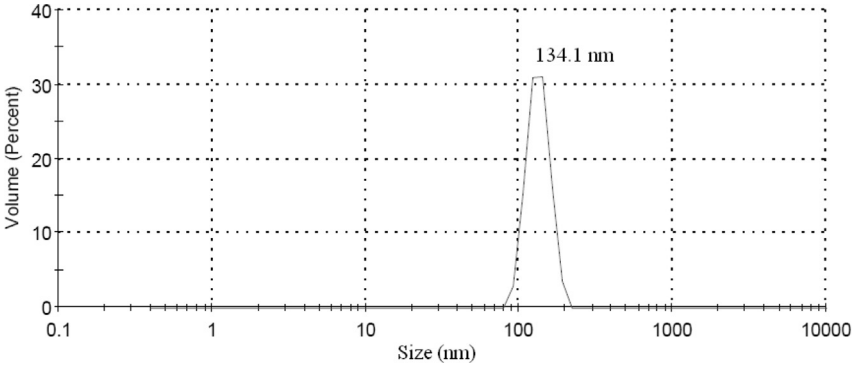

Fig. 2 – Particle size distribution for the synthesized ZrP particles measured at 30 °C and 60% RH.

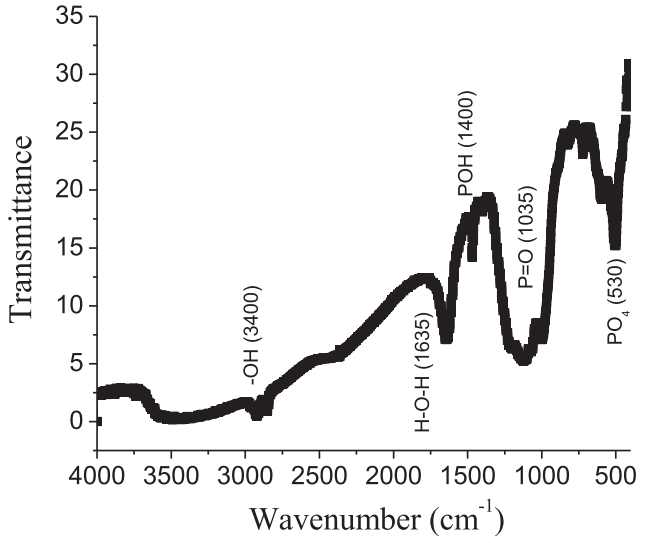

Fig. 3 – FT-IR spectra for the synthesized ZrP powder measured at 30 °C and 60% RH.

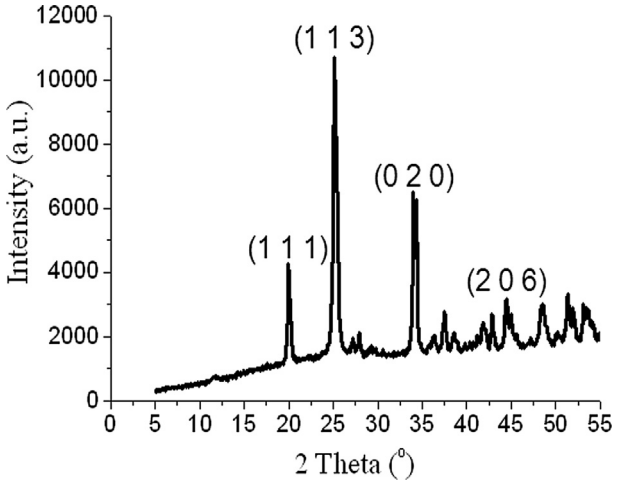

Fig. 4 – XRD patterns for the synthesized ZrP powder measured at 30 °C and 60% RH.

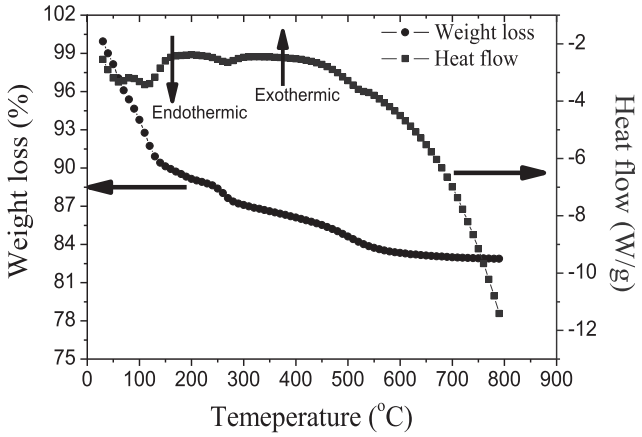

Fig. 5 – TGA/DSC curve for the synthesized ZrP powder.

throughout the surface which indicates proper impregnation of the ZrP particles on the PVDF support. The membrane was also crack free and no defects were found for all the magnifications used. Fig. 7(d) shows cross view of the membrane and the thickness of the membrane was measured to be 60 μm.

The SEM-EDS image and spectrum for the top surface and cross-section of the ZrP/PVDF membrane are shown in Fig. 8 (a) and (b) respectively. Large peaks for C and F were due to the PVDF support and the presence of Zr and P elements indicated the presence of ZrP in the membrane. Table 1 summarizes the atomic percentages of all the elements present in the top surface and cross-section of the synthesized membrane. The results show that the atomic percentage of the Zr and P are higher in the cross-section of the membrane compared to the top surface of the membrane. This confirms that the formation of ZrP is inside the pores of the PVDF support.

TGA

High thermal stability of the membrane is desirable for DMFC operation at elevated temperatures. Water retention capacity at elevated temperature is even more desired because the proton conductivity is strongly correlated to the water content of the membrane. TGA curves of ZrP/PVDF membrane and Nafion-117 are shown in Fig. 9. Initial weight loss up to 100 °C, a region associated with loss of surface water and volatiles, for the synthesized membrane was around 2–3% and it was slightly lower than Nafion-117. However, ZrP/PVDF membrane showed appreciable weight loss (8%) up to 200 °C while there was practically no weight loss for Nafion-117. The weight loss for ZrP/PVDF membrane was due to the loss of structurally bound water associated with ZrP particles. TGA result indirectly shows the moisture retention capacity for the ZrP/PVDF membranes at temperatures higher than Nafion-117. The higher water retention for the membrane is in agreement with results mentioned in Fig. 5 where ZrP particles showed excellent thermal stability and good water holding capacity even at elevated temperatures. For ZrP/PVDF membrane, major weight loss occurred at 420 °C, which can be attributed to the decomposition of polymeric chain of the PVDF support [17]. On the other hand, Nafion-117 showed almost same decomposition temperature with negligible residual weight in comparison to the synthesized membrane (60%). The membrane is thermally stable up to 380 °C. Compared to this, Nafion-117 has thermal stability only up to 350 °C.

Tensile test

The stress–strain curves of ZrP/PVDF and Nafion-117 membranes in dry state are shown in Fig. 10. Compared to Nafion-117 (34 MPa), the synthesized membrane ZrP/PVDF showed higher tensile strength (41 MPa). The higher tensile strength is due to PVDF backbone of the membrane.

Oxidative stability test

Fenton's reagent test is an accelerated oxidative stability test that measures resistance of membrane to the attack of the radical species (OH• and OOH•) which are known to get generated at the electrodes of DMFC. Fig. 11 shows the percentage retained weight of the membrane at different immersion times. Loss in weight of the ZrP/PVDF membrane after 24 h was only 5.1% compared to 6.1% weight loss shown by Nafion-117 under identical conditions. The oxidative

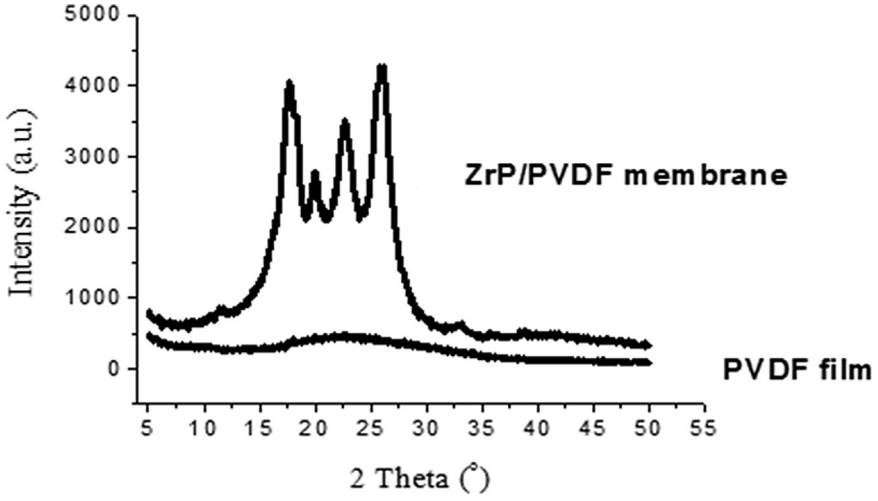

Fig. 6 – XRD patterns of PVDF film and ZrP/PVDF membrane measured at 30 °C and 60% RH.

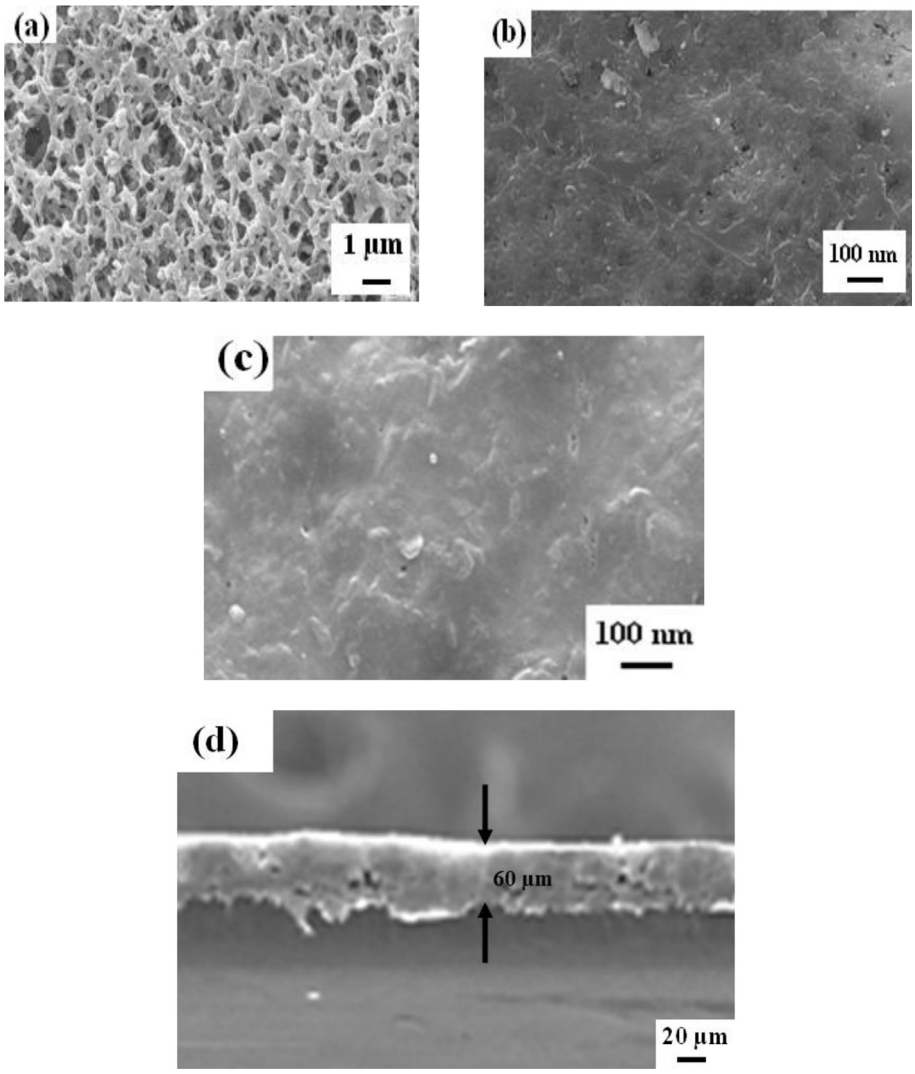

Fig. 7 – SEM images of (a) PVDF film, ZrP/PVDF membrane obtained after impregnation times of (b) 12 h, (c) 48 h and (d) cross-sectional view.

stability of the membrane is superior to Nafion-117. It is reported [18] that the oxidative degradation of the membrane starts from the sulfonic acid function groups of the membrane that provide ion exchanging capacity to the membrane. It is for this reason that the oxidative stability of non-fluorine hydrocarbon backbone types of membrane is even lower than Nafion-117. Increase in density of ion-exchanging functional groups is desired for improving ion-selectivity and proton conductivity of membrane, but it also leads to lowering of the oxidative stability of the membrane. The synthesized membrane consists of inorganic ion exchangers which are not affected by Fenton's reagent. The loss in weight of the synthesized membrane is primarily due to attack on the PVDF support. Inorganic-organic ion exchange membrane therefore provides an alternative way of ion exchange membrane synthesis where increase in density ion-exchanging groups does not affect the oxidative stability of membrane adversely. During the entire test the membrane sample did not break which shows the superior chemical stability of the synthesized membrane.

Water and methanol uptake

Water uptake, a measure of water holding capacity of a membrane, is essential for protonic conductivity of the membrane. Water uptake was 28.7% for ZrP/PVDF membrane. For Nafion-117, the water uptake (29.6%) was slightly higher compared to the ZrP/PVDF membrane.

Methanol uptake of the ZrP/PVDF membrane (8.5%) was much lower than the Nafion-117 membrane (16.5%). Lower methanol uptake for the membrane was due to presence of inorganic ZrP phase in the membrane. In fact, it has been reported in literature [19] that methanol permeability of Nafion-117 could be reduced by doping it with ZrP.

Transport number and IEC

Membrane potential, the potential difference between electrolyte solutions of different concentrations separated by an ion-exchange membrane, develops due to difference in counter-ion and co-ion concentration in the membrane phase. Its magnitude is determined by co-ion exclusion which in turn is determined by surface charge density of the

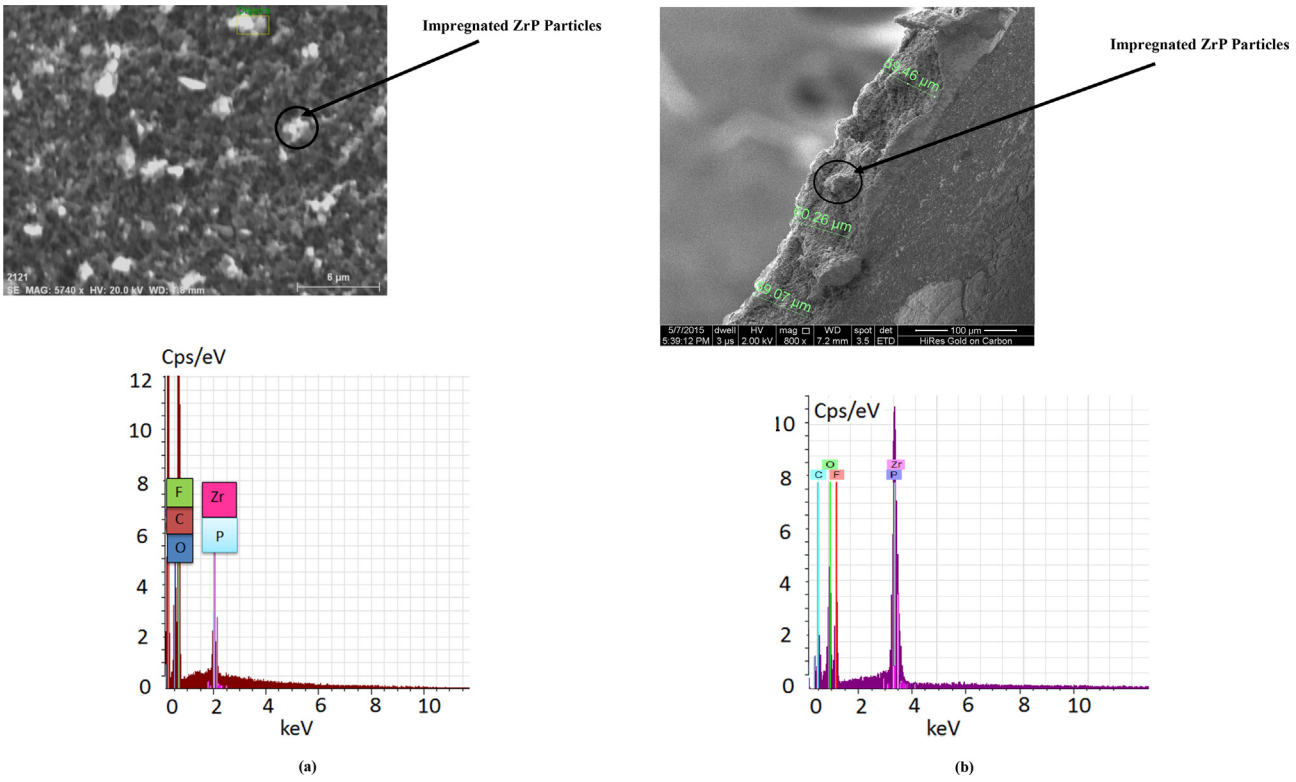

Fig. 8 – The SEM-EDS image and spectrum for (a) top surface and (b) cross-section of ZrP/PVDF membrane.

Table 1 – EDS elemental analysis of the top surface and cross section of ZrP/PVDF membrane.

Element	Atomic percentage	
	Top surface	Cross-section
C	44.79	26.72
F	36.69	43.22
O	15.66	17.14
P	2.00	8.17
Zr	0.86	4.75

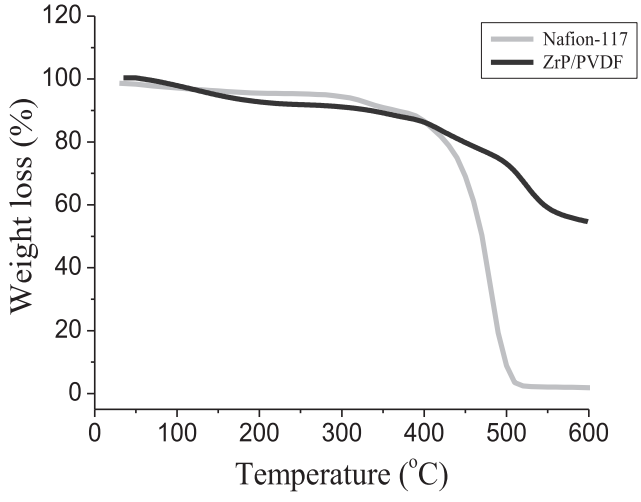

Fig. 9 – TGA curves for ZrP/PVDF membrane and Nafion-117.

membrane [11]. Membrane potential can also be used to calculate transport number of counter-ion. Na^+ transport number was 0.85 for ZrP/PVDF membrane and the value is low comparable with 0.96 value for the Nafion-117 membrane.

IEC measures the total number of ion exchangeable sites present in the membrane and is another electrochemical method for estimating the surface charge of the membrane.

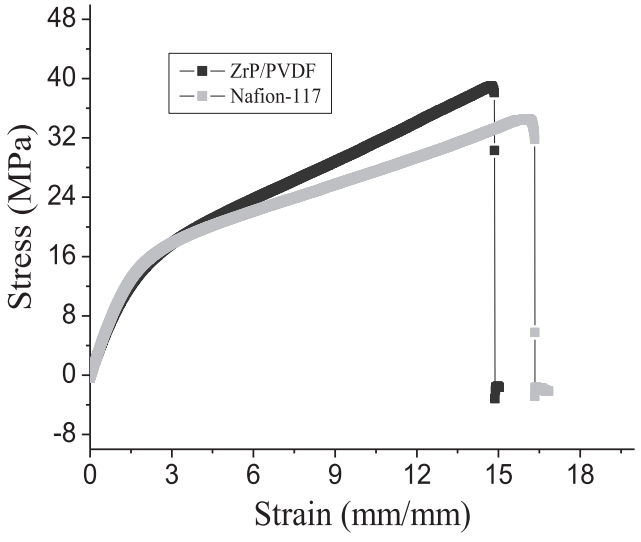

Fig. 10 – Stress–strain curve for (a) ZrP/PVDF and (b) Nafion-117 membrane measured in the dry state at 30 °C and 60% RH.

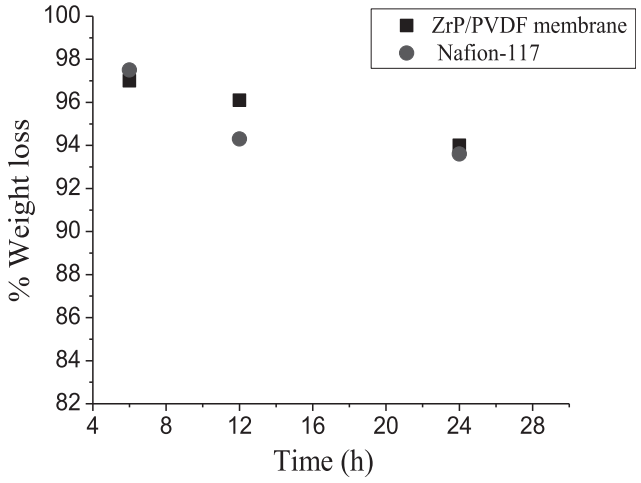

Fig. 11 – Oxidative stability for the synthesized membrane and Nafion-117 under Fenton's test.

IEC of the ZrP/PVDF membrane was 0.76 meqg^{-1} which is lower than Nafion-117 (0.9 meqg^{-1}).

Proton conductivity

Proton conductivity of the synthesized ZrP/PVDF membrane calculated from the impedance measurement and thickness of the membrane (60 μm), was 1.25 mScm^{-1}. This correlates well with the lower water uptake of the membrane and it is well known that water plays an important role in proton conductivity. Although the proton conductivity of ZrP/PVDF membrane was much lower than that of Nafion-117 (13 mScm^{-1}) but the difference in the areal resistances of the two membrane was less (1.35 Ω-cm^2 for Nafion-117 and 4.8 Ω-cm^2 for ZrP/PVDF membrane). Fig. 12 (a) compares proton conductivity and areal resistance for ZrP/PVDF membrane, Nafion-115 and Nafion-117. Though the Proton conductivity of the ZrP/PVDF membrane was low at 30 °C, but, as shown in Fig. 12 (b), it increased nearly four-fold to 5.2 mS cm^{-1} at 60 °C. This indicated, that while the membrane may perform poorly in DMFC at low temperature (around room temperature) compared to Nafion membrane, the performance at high temperature may be comparable.

Compared to polymeric membranes like Nafion, SPEEK, s-PBI etc., the reported proton conductivity for the synthesized ZrP/PVDF membrane is considerably lower but was higher than other ZrP based composite membranes used in DMFC. Peighambardoust et al. [19] reported proton conductivity of 3–4 mScm^{-1} at 60 °C for the ZrP based composite membrane measured. Helen et al. [20] have also reported the proton conductivity of the ZrP based composite membrane in the range of 2.2–2.7 mScm^{-1} between 70 °C and 90 °C.

Methanol permeability

Methanol permeability for the ZrP/PVDF and Nafion membranes, measured at room temperature (30 °C), is shown in Fig. 13. Methanol permeability of ZrP/PVDF membrane (4.1 × 10^{-7} cm^2 s^{-1}) was lower than both Nafion-115 (11.8 × 10^{-7} cm^2 s^{-1}) and Nafion-117 (12.8 × 10^{-7} cm^2 s^{-1}) [21,22] and this correlates well with the lower methanol uptake of ZrP/PVDF compared to Nafion-117. A lower methanol

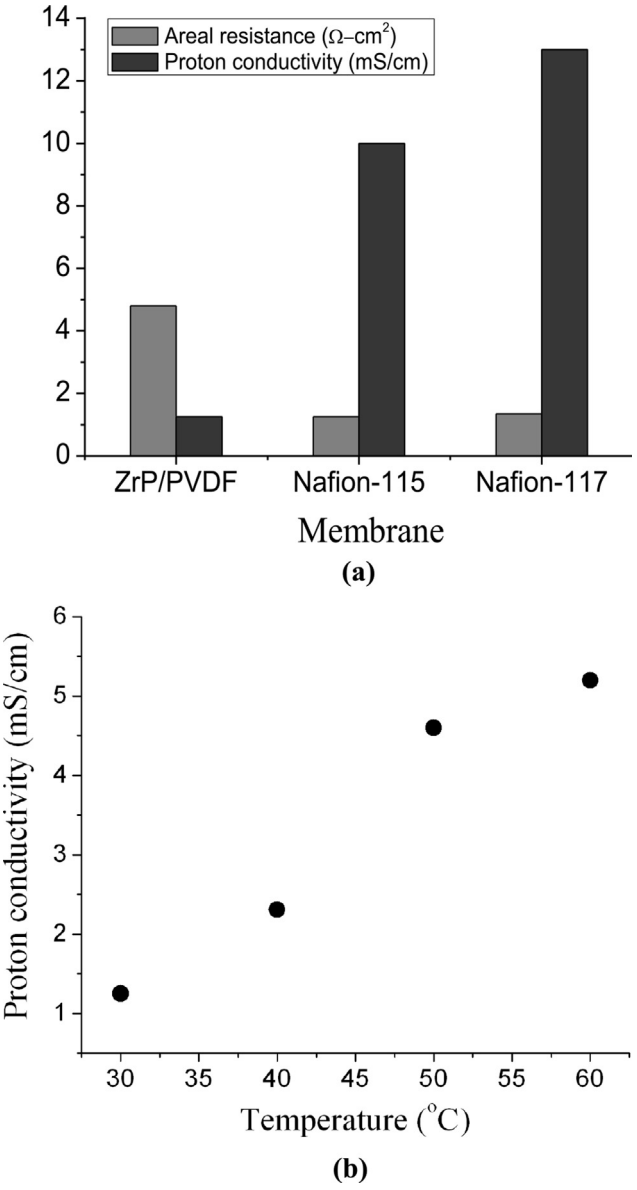

Fig. 12 – (a) Proton conductivity and areal resistance for the ZrP/PVDF and Nafion membranes measured at 30 °C and 60% RH and (b) effect of cell temperature on the proton conductivity of the membrane.

permeability/crossover increases the DMFC's EMF and thereby improves the performance of the DMFC. Moreover, it also improves the fuel efficiency of the DMFC by reducing loss of methanol fuel from anode side to cathode side of the cell.

DMFC performance

Single cell DMFC test

OCV for cell with ZrP/PVDF membrane was 0.700 V which was higher than OCV obtained for the cell with Nafion-117 (0.665 V) at identical conditions (35 °C and 60% RH). This was due to lower methanol permeation through ZrP/PVDF membrane. Polarization curve for the single cell DMFCs with the two membranes is shown in Fig. 14. For cell with ZrP/PVDF membrane, activation overpotential dominated region was

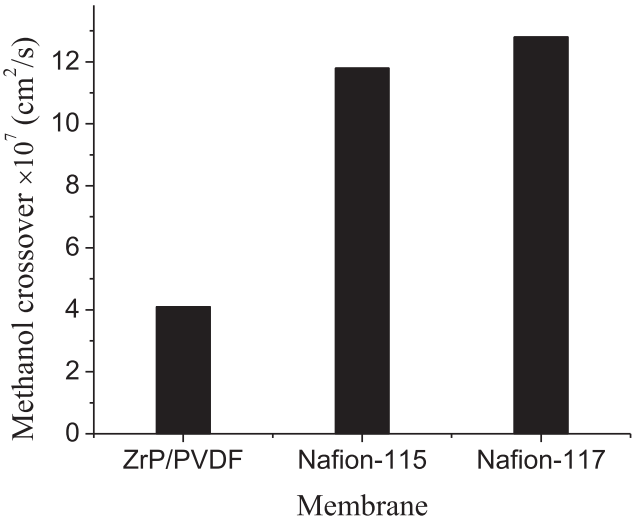

Fig. 13 – Methanol crossover for the ZrP/PVDF and Nafion membranes measured at 30 °C and 60% RH.

restricted to lower current densities (up to 20 $mAcm^{-2}$). Ohmic overpotential dominated region, characterized by linear drop in cell potential with current density, was obtained up to 42 $mAcm^{-2}$. At higher current densities, sharp fall in cell potential indicated concentration overpotential dominated regime [23]. Maximum power density of 23.7 $mWcm^{-2}$ was obtained at 50 $mAcm^{-2}$ and 0.475 V. Maximum current density for cell with ZrP/PVDF membrane was 70 $mAcm^{-2}$. Higher OCV and power density was achieved compared to the other ZrP based composite membranes reported in literature. Helen el al. [24] reported only 6 $mWcm^{-2}$ peak power density and 16 $mAcm^{-2}$ maximum current density at room temperature.

DMFC with Nafion-117 membrane achieved peak power density of 30.5 $mWcm^{-2}$ at 70 $mAcm^{-2}$ and 0.436 V. Also the maximum current density was higher for Nafion-117 (83 $mAcm^{-2}$).

Effect of operating parameters

Effect of temperature, methanol concentration and relative humidity on DMFC performance was determined by independently varying values of these parameters.

Effect of temperature

The cell temperature was varied from 30 °C to 60 °C keeping the methanol concentration fixed at 1 M with 60% relative humidity of air. Fig. 15 shows the performance of DMFC with ZrP/PVDF membrane at different temperatures (30–60 °C). OCV increased from 0.680 V to 0.739 V, with increase in temperature from 30 °C to 60 °C due to enhanced electrode kinetics at elevated temperature [25]. Peak power density increased substantially from 18.5 $mWcm^{-2}$ (at cell voltage of 0.403 V) at 30 °C to 32.3 $mWcm^{-2}$ (at the cell voltage of 0.539 V) at 60 °C. Similarly, maximum current density increased from 61 $mAcm^{-2}$ at 30 °C to 72 $mAcm^{-2}$ at 60 °C.

Effect of methanol concentration

Methanol concentration was varied from 0.5 M to 2 M keeping the cell temperature fixed at 30 °C with 60% relative humidity of air. Fig. 16 shows the DMFC polarization curves for different concentrations of methanol in the anode feed solution. OCV of the cell increased from 0.615 V to 0.680 V as the methanol concentration was increased from 0.5 M to 1 M. This indicated that the methanol crossover was not prominent even at higher methanol concentration. However, OCV decreased slightly with further increase in the methanol concentration to 2 M. Peak power density increased from 17.6 $mWcm^{-2}$ (at cell voltage 0.411 V) to 18.5 $mWcm^{-2}$ (at a cell voltage of 0.403 V) as methanol concentration was increased from 0.5 to 1 M and then decreased to 17.5 $mWcm^{-2}$ (at cell voltage of 0.429 V) as methanol concentration was further increased to 2 M. However, the maximum achieved current density was same for 0.5 M (60 $mAcm^{-2}$) and 2 M (61 $mAcm^{-2}$) methanol concentration. In contrast, for DMFC with Nafion-117 membrane, performance deterioration is reported as methanol concentration is increased to 1 M [26].

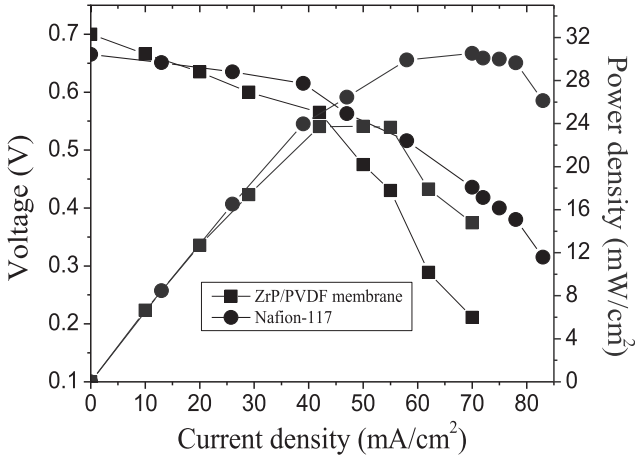

Fig. 14 – DMFC performance for the ZrP/PVDF and Nafion-117 membranes measured at 35 °C and 60% relative humidity.

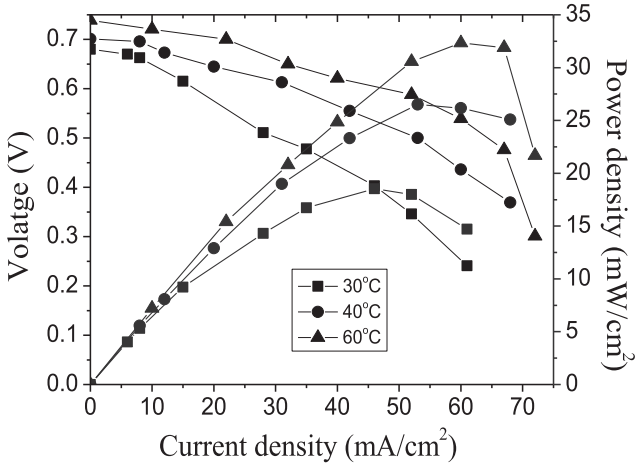

Fig. 15 – Effect of temperature on the DMFC performance measured at 60% RH and 1 M methanol concentration.

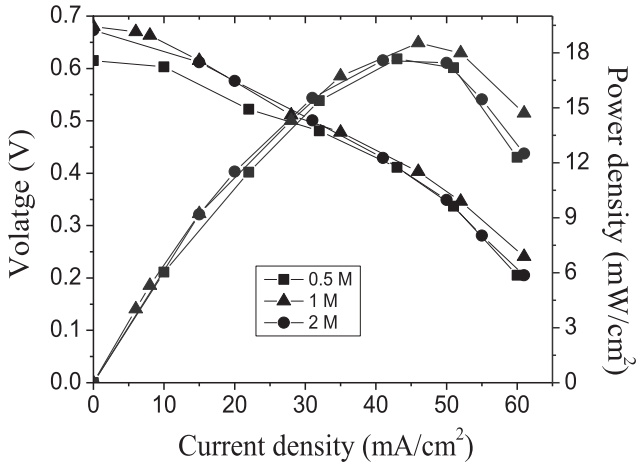

Fig. 16 – Effect of methanol concentration on the DMFC performance measured at 30 °C and 60% RH.

Effect of relative humidity

The relative humidity of the air was varied from 40 to 60% keeping the cell temperature fixed at 30 °C with methanol concentration 1 M. Fig. 17 shows the polarization curves of DMFC with ZrP/PVDF membrane at different relative humidities (40–60%) of air flowing through the cathode. OCV increased from 0.615 V for 40% relative humidity to 0.68 V for air with 60% relative humidity. However, there was a slight drop in OCV (0.676 V) with further increase in the relative humidity to 90%. Peak power density was 17 mWcm^{-2} (at cell voltage of 0.405 V) for 40% relative humidity and it increased to 18.5 mWcm^{-2} (at a cell voltage of 0.403 V) for 60% relative humidity while it was 18.2 mWcm^{-2} (at a cell voltage of 0.444 V) for 90% relative humidity. The maximum achieved current density at 40% relative humidity was 61 mAcm^{-2}, almost same as 60 mAcm^{-2} at 90% relative humidity.

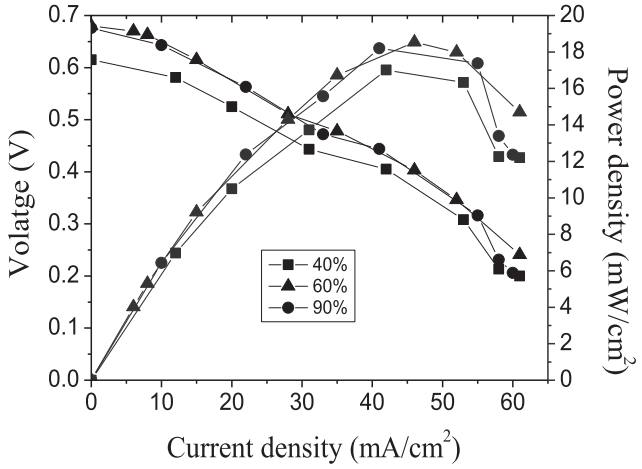

Fig. 17 – Effect of relative humidity on the DMFC performance measured at 30 °C and 1 M methanol concentration.

Conclusion

A proton conducting ZrP/PVDF ion exchange membrane was synthesized for DMFC. Presence of protons attached to P=O group was confirmed by ^{1}H NMR and the shifts in the FT-IR peaks of the characteristic functional groups. SEM micrographs of the membrane showed defect-free top surface with pores of support completely filled with sized particles of ZrP. XRD pattern indicated the presence of crystalline phase in the membrane. The thermal stability of the membrane was superior to Nafion-117 with higher mechanical strength in the dry state. Water to methanol uptake ratio was higher due to PVDF support which has low selectivity for methanol. Membrane possessed fair electrochemical properties, 0.85 static counter-ion transport number, 0.76 meqg^{-1} IEC and 1.25 mScm^{-1} proton conductivity at 30 °C. Methanol crossover through the membrane was much lower than Nafion-117 due to lower methanol uptake. The DMFC performance at 35 °C was much better than the reported values of ZrP based membranes. However, it was inferior to Nafion-117 because of poor proton conductivity but better DMFC performance at elevated temperature is expected due to the enhanced proton conductivity. The best DMFC performance was obtained at 60 °C cell temperature, 1 M methanol concentration and 60% relative humidity.

REFERENCES

[1] Kamarudin SK, Ahmad F, Daud WRW. Overview on application of direct methanol fuel cell (DMFC) for portable electronic devices. Int J Hydrogen Energy 2009;34:6902–16.
[2] Alberti G, Casciola M, Capitani D, Donnadio A, Narducci R, Pica M, et al. Novel Nafion–zirconium phosphate nanocomposite membranes with enhanced stability of proton conductivity at medium temperature and high relative humidity. Electrochim Acta 2007;52:8125–32.
[3] Clearfield A. Role of ion exchange in solid state chemistry. Chem Rev 1988;88:125–48.
[4] Raposo CMO, Eon JG. On the nature of sandwiched chromium complexes in exchanged α-zirconium phosphate. Mater Res 2002;5:421–6.
[5] Thakkar R, Chudasama U. Synthesis, characterization and proton transport property of crystalline–zirconium titanium phosphate, a tetravalent bimetallic acid salts. J Sci Ind Res 2009;68:312–8.
[6] Nagarale RK, Shin W, Singh PK. Progress in organic-inorganic composite membranes for fuel cell applications. Polym Chem 2010;1:388–408.
[7] Alberti G, Casciola M, Palombari M. Inorgano-organic proton conducting membranes for fuel cells and sensors at medium temperatures. J Membr Sci 2000;172:233–9.
[8] Grot WG, Rajendran G. Membranes containing inorganic and membrane and electrode assemblies and electrochemical cells employing same. U. S Patent 5,919,583 1999.
[9] Si Y, Kunz HR, Fenton JM. Nafion-Teflon-Zr(HPO$_4$)$_2$ composite membranes for high-temperature PEMFCs. J Electrochem Soc 2004;151:A623–31.
[10] Yang C, Srinivasan S, Arisco AS, Creti P. Composite Nafion/zirconium phosphate membranes for direct methanol fuel cell operation at high temperature. Electrochem Solid State Lett 2001;4:A31–4.

[11] Zuo X, Yu S, Xu X, Bao R, Xu J, Qu W. Preparation of organic-inorganic hybrid cation-exchange membranes via blending method and their electrochemical characterization. J Membr Sci 2009;328:23–30.
[12] Vetter S, Ruffmann B, Buder I, Nunes SP. Proton conducting membranes of sulfonated poly (ether ketone ketone). J Membr Sci 2005;260:181–6.
[13] Duangkaew P, Wootthikanokkhan J. Methanol permeability and proton conductivity of direct methanol fuel cell membranes based on sulfonated poly (vinyl alohol)- Layered silicate nanoparticles. J Appl Polym Sci 2008;109:452–8.
[14] Kong X. Characterization of proton exchange materials for fuel cells by solid state nuclear magnetic resonance. Graduate Theses and Dissertations. 2010. Paper 11912.
[15] Horsley SE, Nowell DV, Stewart DT. The infrared and Raman spectra of α-zirconinm phosphate. Spectrochim Acta A 1974;30:535–41.
[16] Slade RCT, Knowles JA, Jones DJ, Roziere J. The isomorphous acid salts α-$Zr(HPO_4)_2.H_2O$, α-$Ti(HPO_4)_2.H_2O$ and α-$Zr(HAsO_4)_2.H_2O$ comparative thermochemistry and vibrational spectroscopy. Solid State Ionics 1997;96:91–109.
[17] Liu F, Yi B, Xing D, Yu J, Zhang H. Nafion/PTFE composite membranes for fuel cell applications. J Membr Sci 2003;212:213–23.
[18] Zhang L, Mukherjee S. Investigation of durability issues of selected non-fluorinated polymer exchange membranes for fuel cell applications. J Elcetrochem Soc 2006;153:A1062–72.
[19] Peighambardoust SJ, Rowshanzamir S, Amjadi M. Review of the proton exchange membranes for fuel cell applications. Int J Hydrogen Energy 2010;35:9349–84.
[20] Helen M, Viswanathan B, Murthy SS. Synthesis and characterization of composite membranes based on α-zirconium phosphate and silicotungstic acid. J Membr Sci 2007;292:98–105.
[21] Chen L, Yu TL, Lin HL, Yeh SH. Nafion/PTFE and zirconium phosphate modified Nafion/PTFE composite membranes for direct methanol fuel cells. J Membr Sci 2008;307:10–20.
[22] Ahmad H, Kamarudin SK, Harsan UA, Daud WRW. Overview of hybrid membranes for direct methanol fuel-cell applications. Int J Hydrogen Energy 2010;35:2160–75.
[23] Ge J, Liu H. Experimental studies of a DMFC. J Power Sources 2005;142:56–69.
[24] Helen M, Viswanathan B, Murthy SS. Fabrication and properties of hybrid membranes based on salts of heteropolyacid, zirconium phosphate and polyvinyl alcohol. J Power Sources 2006;163:433–9.
[25] Chen S, Ye F, Lin W. Effect of operating conditions on the performance of a direct methanol fuel cell with PtRuMo/CNTs as anode catalyst. Int J Hydrogen Energy 2010;35:8225–33.
[26] Scott K, Taama WM, Argyropoulos P, Sundmacher K. The impact of mass transport and methanol crossover on the direct methanol fuel cell. J Power Sources 1999;83:204–16.